SUPPORTING INFORMATION

High framework metal sites in heteroatom zeolite as Lewis acid catalyst for the conversion of ethanol-acetaldehyde to 1,3-butadiene

Haoxi Jiang, [abc] Liping Yi, [abc] Guochao Yang, [abc] and Lingtao Wang*[abc]

Corresponding Address:

[a] *Key Laboratory for Green Chemical Technology of Ministry of Education, R&D Center for Petrochemical Technology, Tianjin University, Tianjin 300072, China*

[b] *Zhejiang Institute of Tianjin University, Ningbo, Zhejiang, 315201, China*

[c] *State Key Laboratory of Engines, Tianjin University, Tianjin 300072, China*

E-mail: ltwang@tju.edu.cn

Tel: +86-22-27406119

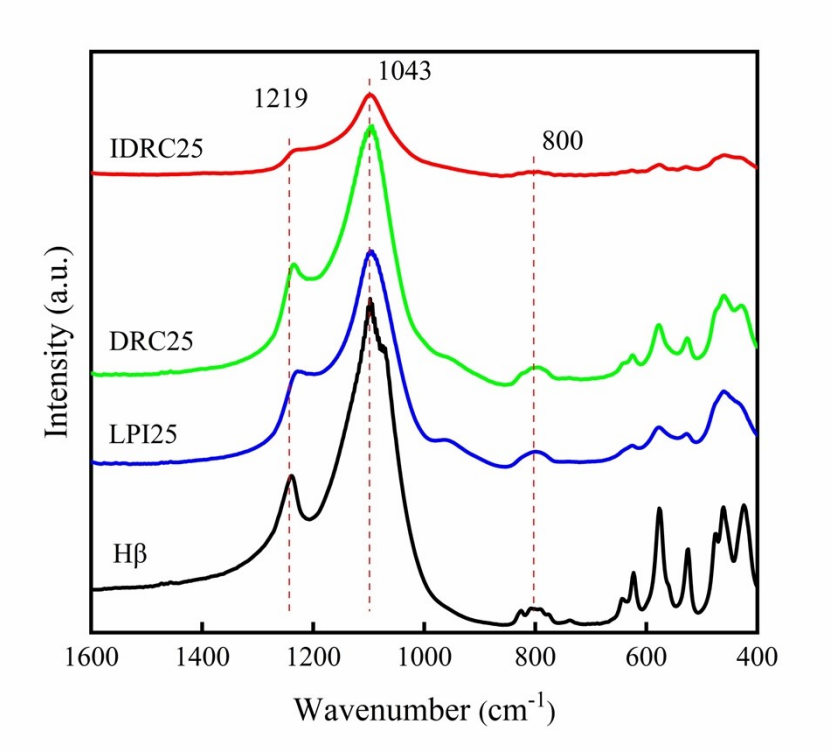

Supplemental Data and Figures

Fig. S1. FI-IR spectra of IDRC25, DRC25 and LPI25. The peaks at 1219, 1043 and 800 cm^{-1} of are attributed to Si-O-Si bond in zeolite framework.

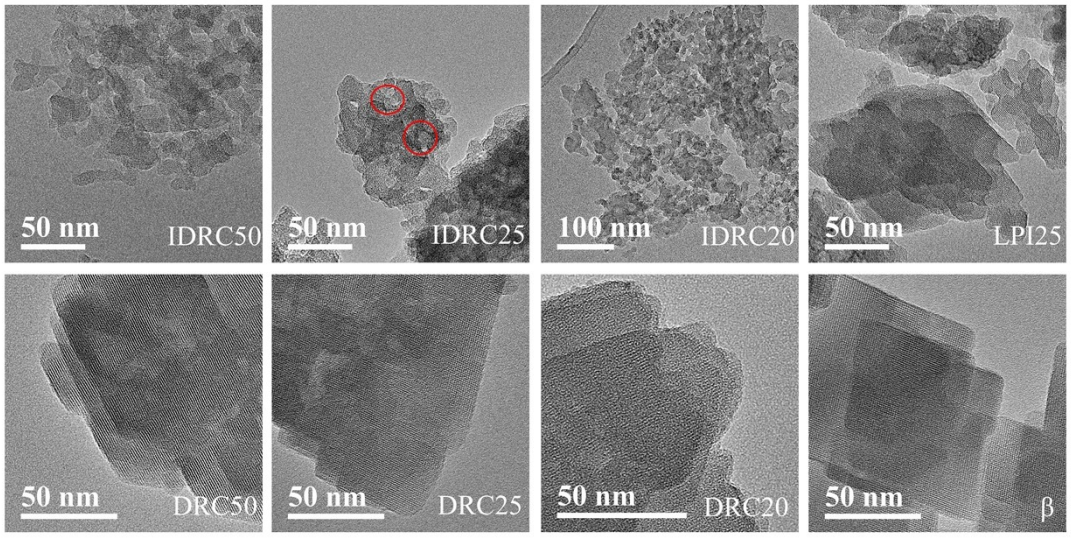

Fig. S2. TEM images of LPI25, samples prepared by IDRC and DRC with different Zr contents.

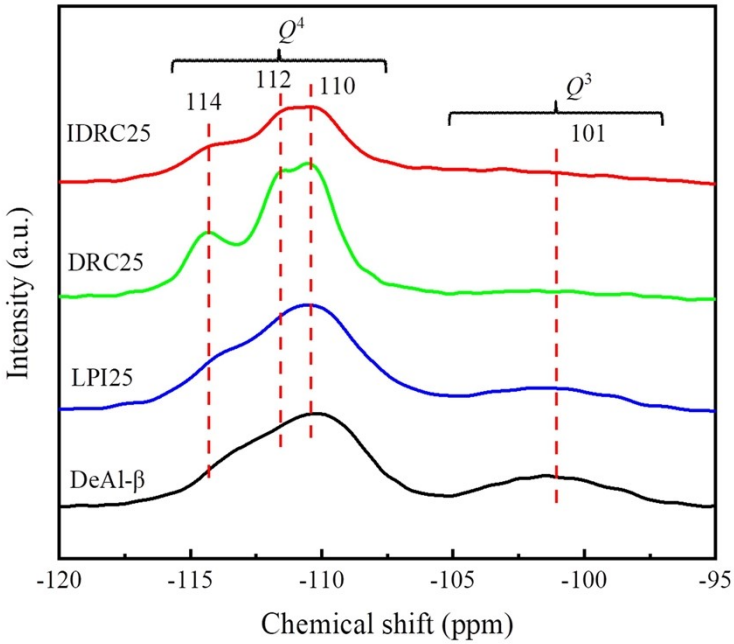

Fig. S3. ^{29}Si MAS NMR spectra of IDRC25, DRC25 and LPI25. The peak at -101 ppm is assigned to Q^3 species of $(SiO)_3SiOH$, and the peaks at -114, -112 and -110 ppm are assigned to Q^4 species of $Si(OSi)_4$ at different T sites.

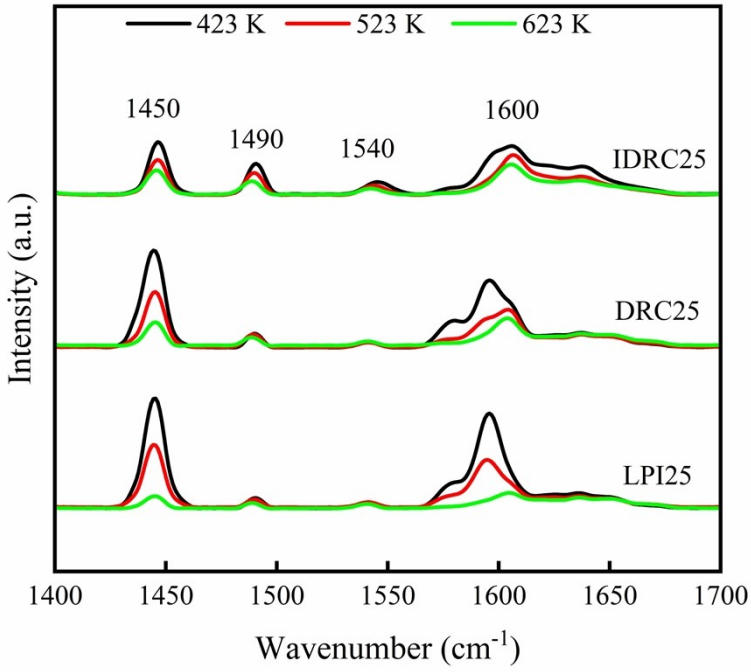

Fig. S4. Py-IR spectra of IDRC25, DRC25 and LPI25. The bands at 1600 and 1450 cm^{-1} are assigned to Lewis acid sites. The band at 1540 cm^{-1} is assigned to Brønsted acid sites. The band at 1490 cm^{-1} represents Brønsted+Lewis sites. The acid strength (weak, medium and strong) was determined by treating at 423, 523 and 623 K.

Table S1. The acidity of samples IDRC25, DRC25 and LPI25 by NH_3-TPD

Sample	Acidity (μmol g^{-1})			Temperature at maximum (K)	
	total	weak	strong	peak 1	peak 2
IDRC25	978	241	737	441	537
DRC25	527	103	424	437	530
LPI25	246	71	174	429	510

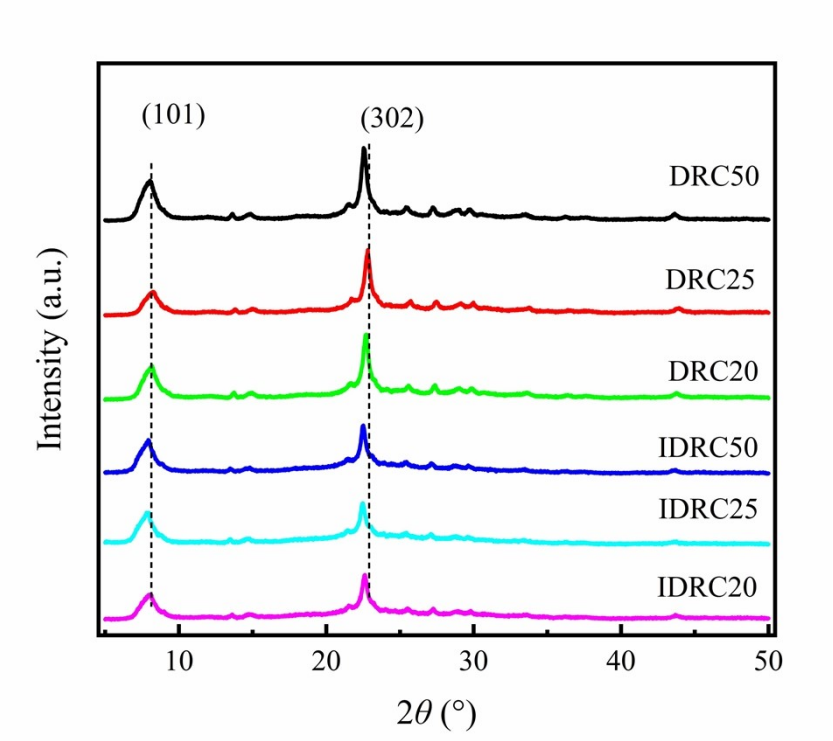

Fig. S5. XRD patterns of IDRC and DRC samples with different Zr contents. The diffraction peaks at 2θ = ~8.0° and 22.4° represents (101) and (302) crystal planes of β zeolite, respectively. ZrO_2 diffraction peaks at 2θ = ~28.5° and 31.8° were not detected in all prepared samples.

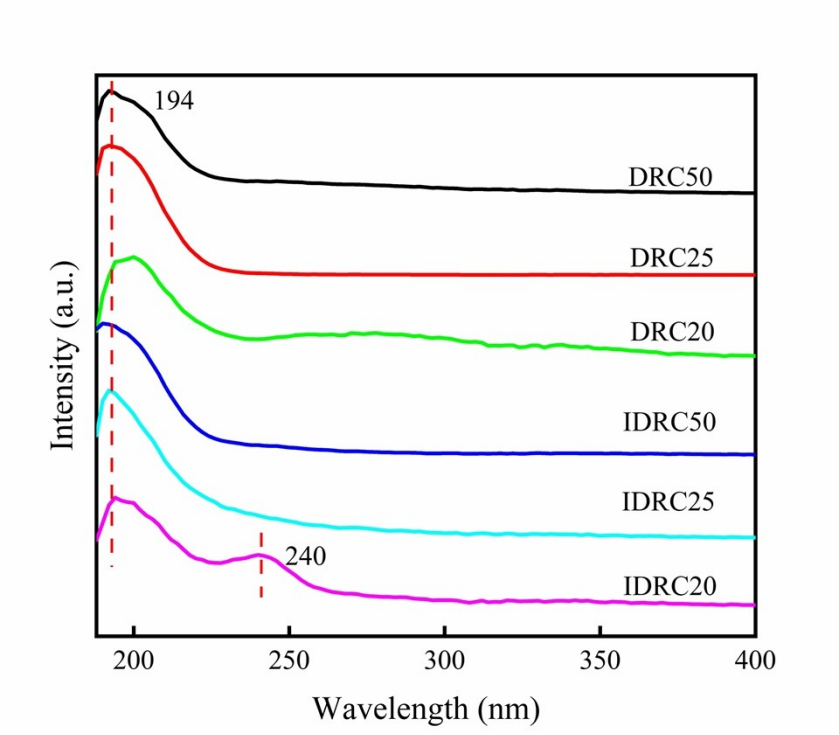

Fig. S6. UV-Vis spectra of IDRC and DRC samples with different Zr contents. The absorption peak at 190-200 nm generally assigns to the tetrahedral Zr in the framework. And the absorption peak at 230-240 nm is related to the extra-framework ZrO_2-like species.

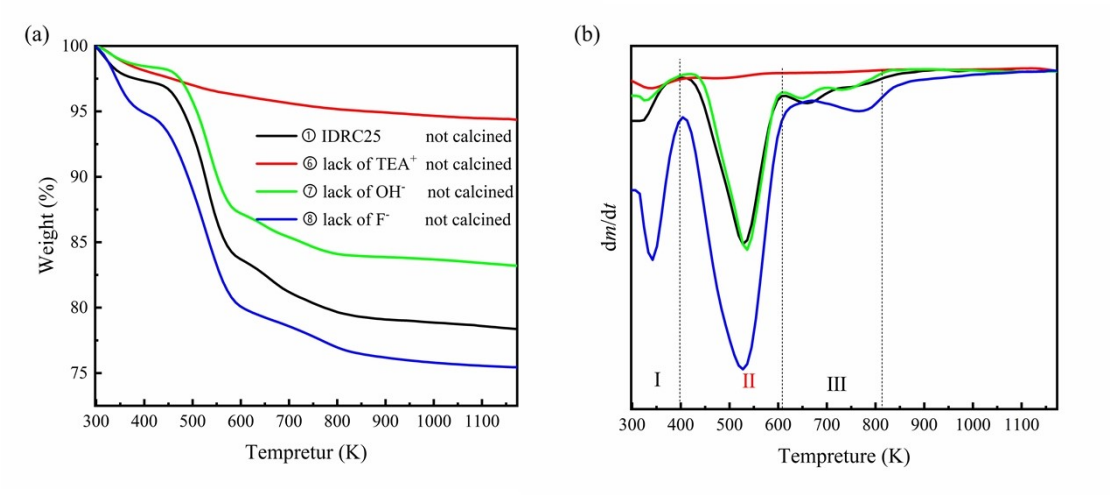

Fig. S7. (a) TG and (b) DTG of comparative experiments. The black line was comparative sample ① IDRC25, red line was sample ⑥ lack of TEA^+, green line was sample ⑦ lack of OH^-, blue line was sample ⑧ lack of F^-. All samples were not calcined. The weight loss in region I (298-423 K) represents the desorption of water in the sample. The region II (423-623 K) represents the Hoffmann elimination of template TEA^+. And the region III (> 623 K) was attributed to the further degradation and oxidation of the template.

Table S2. The textural properties of IDRC and DRC samples with different Zr contents.

Sample	R.C. (%)	V_{Meso} ($cm^3\ g^{-1}$)	Zr content (wt%)		Si/Zr [a]	Con. [b] (%)	Sel. [b] (%)
			gel	Product [a]			
IDRC50	58	0.618	2.9	3.1	46	48.7	58.6
IDRC25	53	0.582	5.6	5.0	28	55.9	66.0
IDRC20	61	0.451	6.9	5.3	26	48.7	58.6
DRC100	114	0.282	1.5	n.m. [c]	n.m. [c]	32.9	63.7
DRC75	114	0.282	2.0	n.m. [c]	n.m. [c]	39.8	64.8
DRC50	102	0.279	2.9	1.35	110	40.7	65.5
DRC25	87	0.285	5.6	2.2	66	45.1	69.4
DRC20	94	0.291	6.9	3.4	43	45.4	66.9
DRC15	80	0.313	8.9	n.m. [c]	n.m. [c]	43.0	62.7

[a] Determined by ICP. [b] Conversion and selectivity. Reaction conditions: 598 K, WHSV = 1.0 h^{-1}, TOS = 6 h. [c] Not measured.

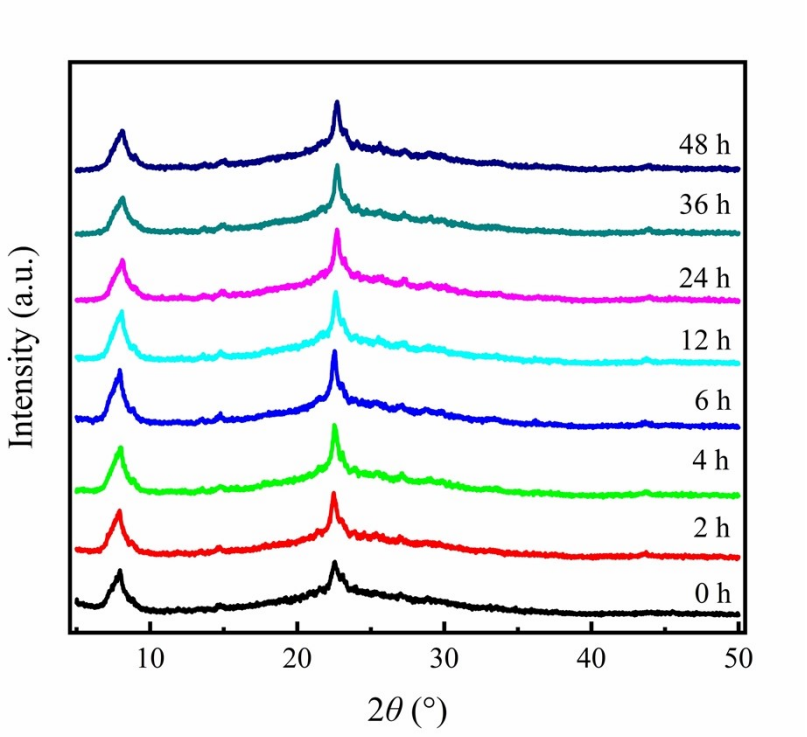

Fig. S8. XRD patterns of IDRC25 crystallized for different time.

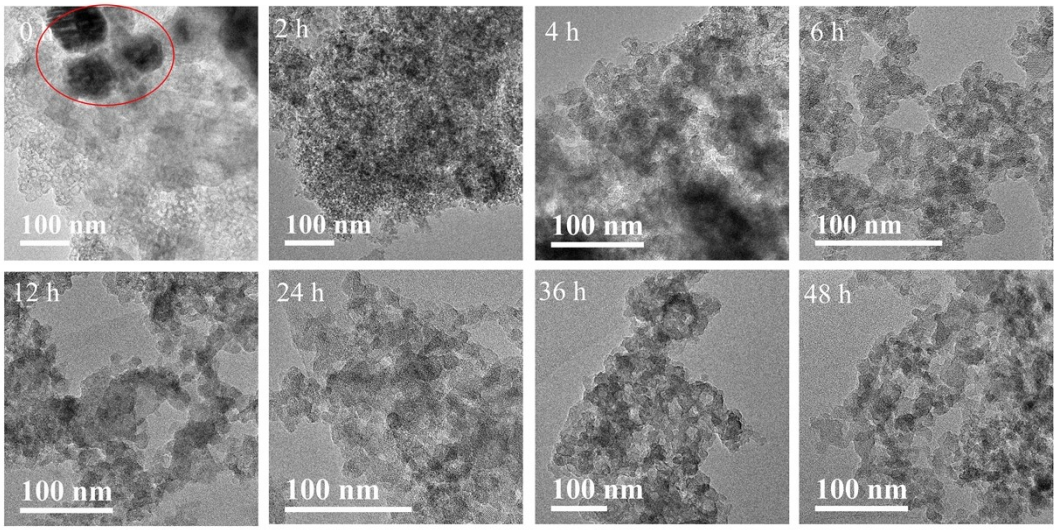

Fig. S9. TEM images of IDRC25 crystallized for different time. The black particles in the red circle are Zr agglomerations in gel.

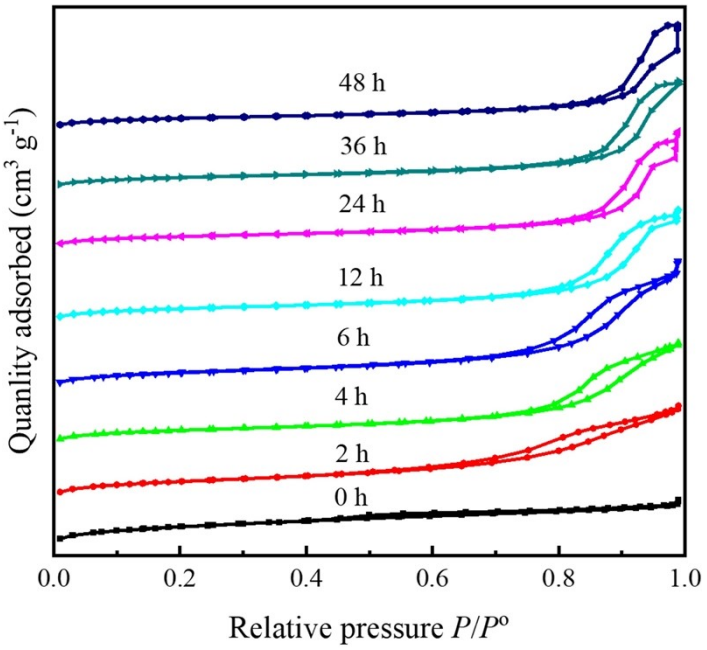

Fig. S10. N_2 adsorption-desorption curves of IDRC25 crystallized for different time.

Table S3. Carbon deposition of IDRC25.

TOS (h)	Carbon deposition (%)
6	13.1
100	25.8